Influence of Hot Plasma Pressure on Magnetodisc Structure at Saturn

N. Achilleos[13], P. Guio[13], C. S. Arridge[23] and N. Sergis[4]

[1]Department of Physics and Astronomy, [2]Mullard Space Science Laboratory, both part of [3]Centre for Planetary Sciences, University College London, UK;
[4]University of Athens **Contact:** nicholas.achilleos@ucl.ac.uk **Download Poster:** http://www.ucl.ac.uk/∼ucapnac/posters/nach_egu_2010.pdf
Acknowledgement: We wish to thank Dr. Nick Sergis and the Cassini MIMI team, who provided the hot plasma pressure moments used in this study.

European Geophysical Union, May 2010

Abstract

We present results of a modelling study undertaken with the UCL Magnetodisc Model in Saturn configuration (Achilleos et al., 2010). The level of hot plasma pressure within the magnetosphere has a strong influence on the magnetic field configuration, under the assumption of force balance in the rapidly rotating plasma. We use a hot plasma index to represent this pressure, and higher values of this parameter lead to a thinner equatorial current sheet and a more radial field. In addition, the magnetic moment of the disc current relative to the planetary dipole moment is affected by hot plasma content, with the model unable to provide static solutions beyond limiting values of the disc moment. We discuss the implications for the range of hot plasma pressures observed within the Kronian environment during the Cassini era.

Introduction

We have investigated the response of the structure of Saturn's magnetosphere to changes in the internal configuration—specifically, the hot plasma content— of the system. We have used the UCL Magnetodisc Model described by Achilleos et al. (2010), which is based on the formalism developed by Caudal (1986) that calculates self-consistent magnetic field and plasma distributions in an axisymmetric, rotating magnetosphere. The computations are based on the assumption of balance between the centrifugal, pressure and magnetic ('$\boldsymbol{J} \times \boldsymbol{B}$') forces on the plasma:

$$\boldsymbol{J} \times \boldsymbol{B} = \nabla P - n_i m_i \omega^2 \rho \boldsymbol{e_\rho}, \tag{1}$$

where $\boldsymbol{J}$, $\boldsymbol{B}$, P, n_i, m_i, and ω respectively denote azimuthal current density, magnetic field, isotropic plasma pressure, ion number density, mean ion mass and plasma angular velocity. ρ is cylindrical radial distance with respect to the planet's magnetic / rotation axis.

Figures 1 and 2 indicate how we have parametrised the hot plasma content of the system using statistical properties of hot pressure moments acquired by the MIMI (Magnetospheric IMaging Instrument) experiment onboard the Cassini spacecraft (e.g. Krimigis et al. (2004)). Achilleos et al. (2010) used a more simplified parametrisation, based on a constant product of hot plasma pressure and unit flux tube volume in the outer magnetosphere – known as the 'hot plasma index' K_h.

Cassini MIMI Observations

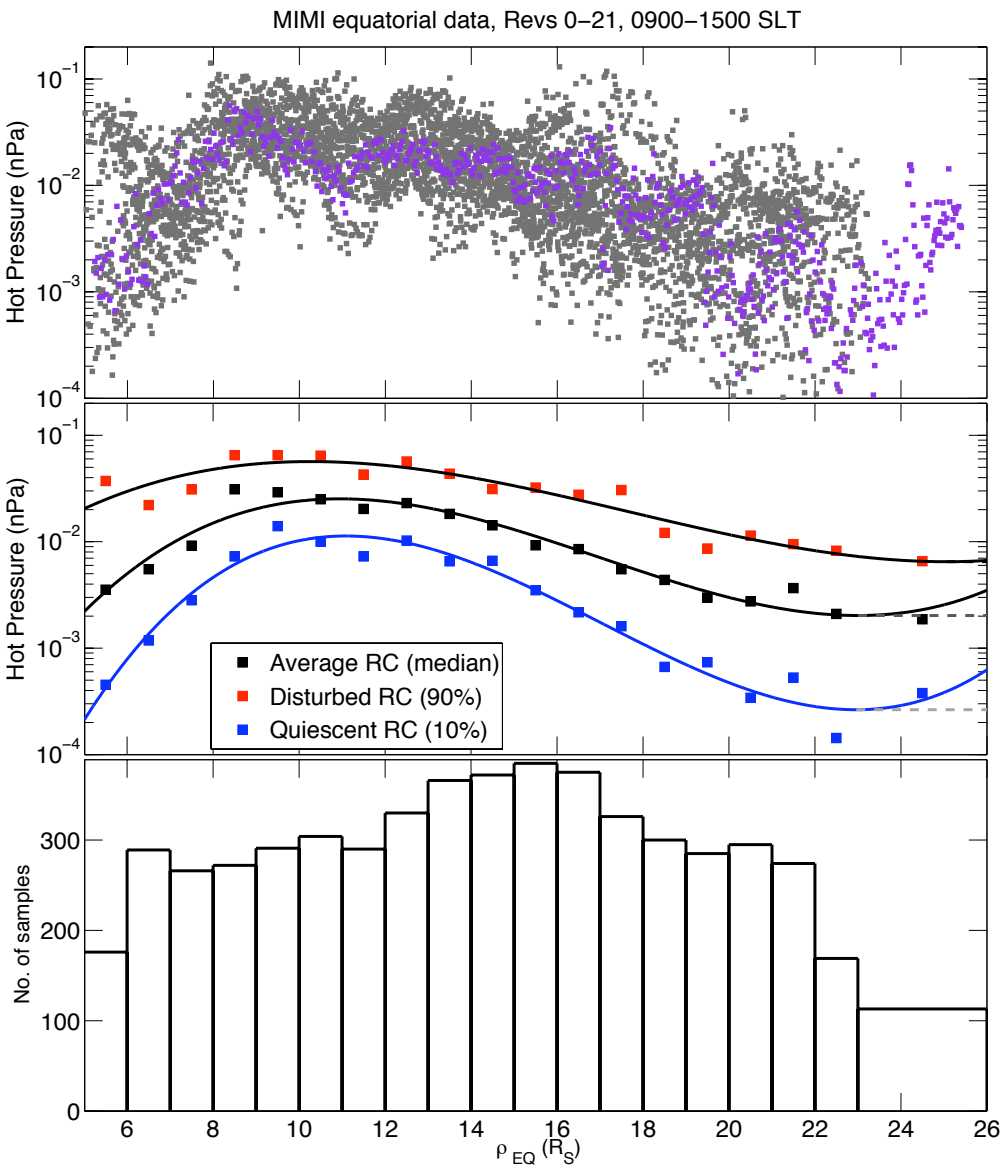

Figure 1: *Top Panel:* Individual pressure moments from the Cassini MIMI experiment, which captures the hot ($>$ 3keV) ion population in Saturn's magnetosphere. Grey points are five-minute samples drawn from the first 23 spacecraft orbits which lie inside the magnetosphere, near the equatorial plane (absolute latitude $|\lambda| < 5°$) and on the dayside (Saturn local time SLT between 09:00 and 15:00). Violet points are drawn from a single orbit, Rev 3 (Feb 14–24, 2005). *Middle Panel*: Median and quantile pressures (see legend) calculated over distance intervals of $\geq$ 1 R_S (Saturn radius, 60300 km). *Bottom Panel*: Number of measurements per interval of ρ_e, the radial distance coordinate in the equatorial plane (with planet centre at zero).

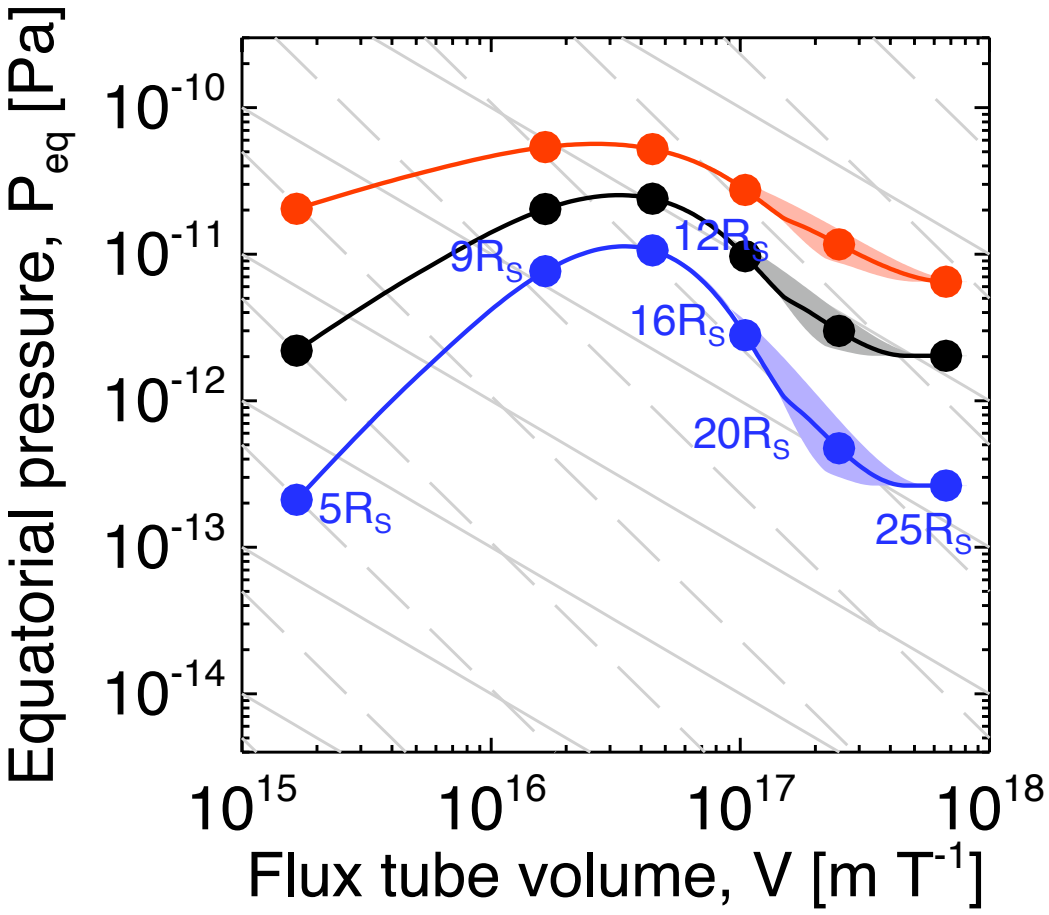

Figure 2: The polynomial fits to equatorial plasma pressure shown in Figure 1 have been used to plot this quantity against the unit flux tube volume, for the three idealised 'ring current states' (similar to the original parametrisation by Sergis et al. (2007)). The outer magnetosphere is characterised by pressure-volume relations similar to both isotherms (solid grey) and adiabats (dashed grey). This feature of the data thus has implications for the nature of radial plasma transport. The flux tube volumes were calculated as described in Achilleos et al. (2010), through the use of the empirical ring current models for Saturn by Bunce et al. (2007), which make use of the original parametrisation by Connerney et al. (1981). 'Smudges' of colour near the nominal curves show the effect of varying the outer edge of this ring current field model, in accordance with conditions at Saturn in the Cassini era inferred by Bunce et al. (2007).

Figure 3: Magnetic Field Models

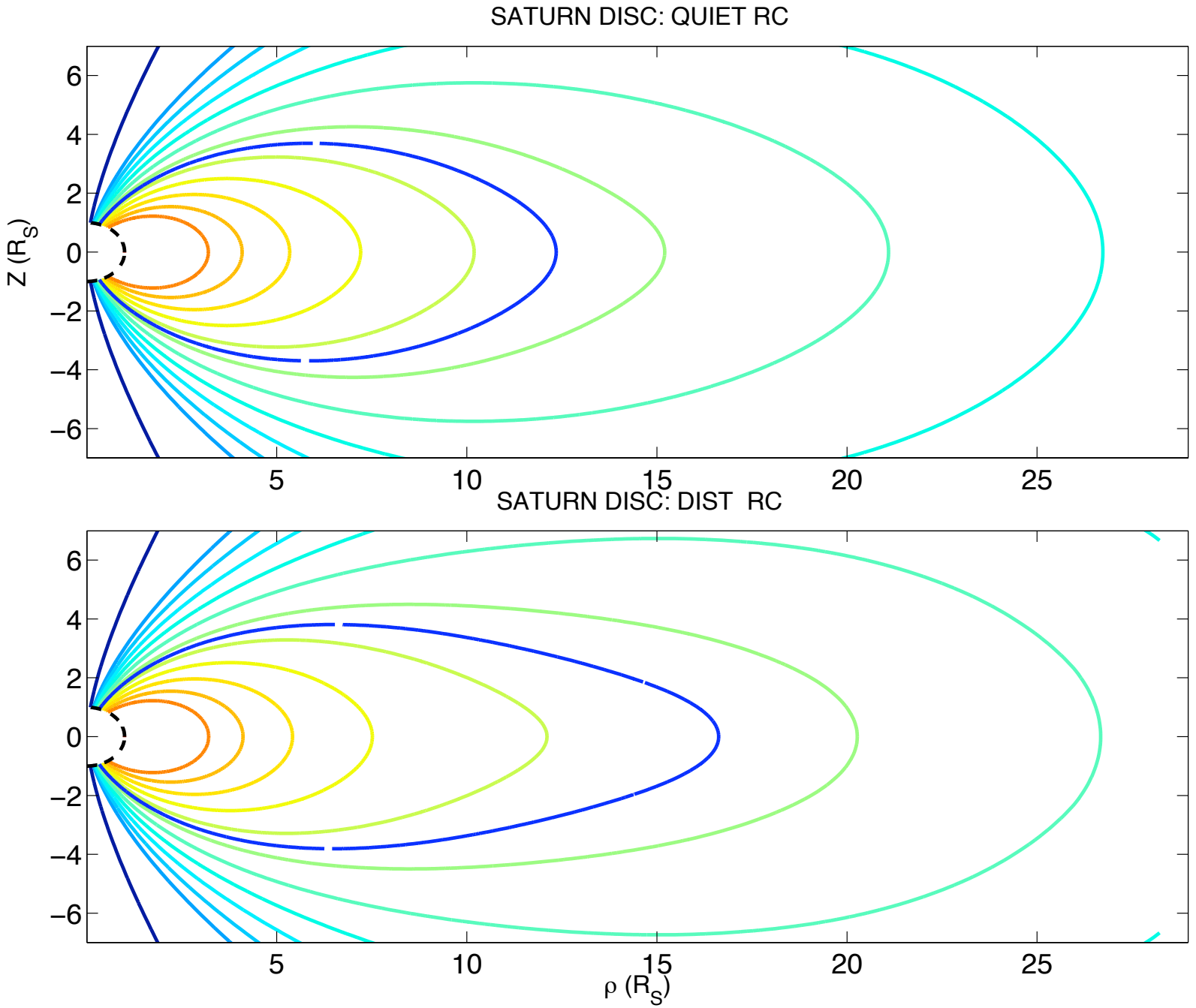

Figure 3, 'Magnetic Field Models': We show magnetic field lines for two different internal configurations of the magnetosphere, corresponding to the idealised 'quiescent' and 'disturbed' ring current states described above. Field lines of the same colour in both panels are 'anchored' to the same latitude in the ionosphere. The field structure becomes more radially 'stretched' and disc-like in response to increased hot plasma pressure. This is partly because the equatorial field lines develop a smaller radius of curvature beyond $\sim 10\ R_S$, in order to balance the increased pressure force with an increased curvature force.

Figure 4: Vertical Pressure Profiles

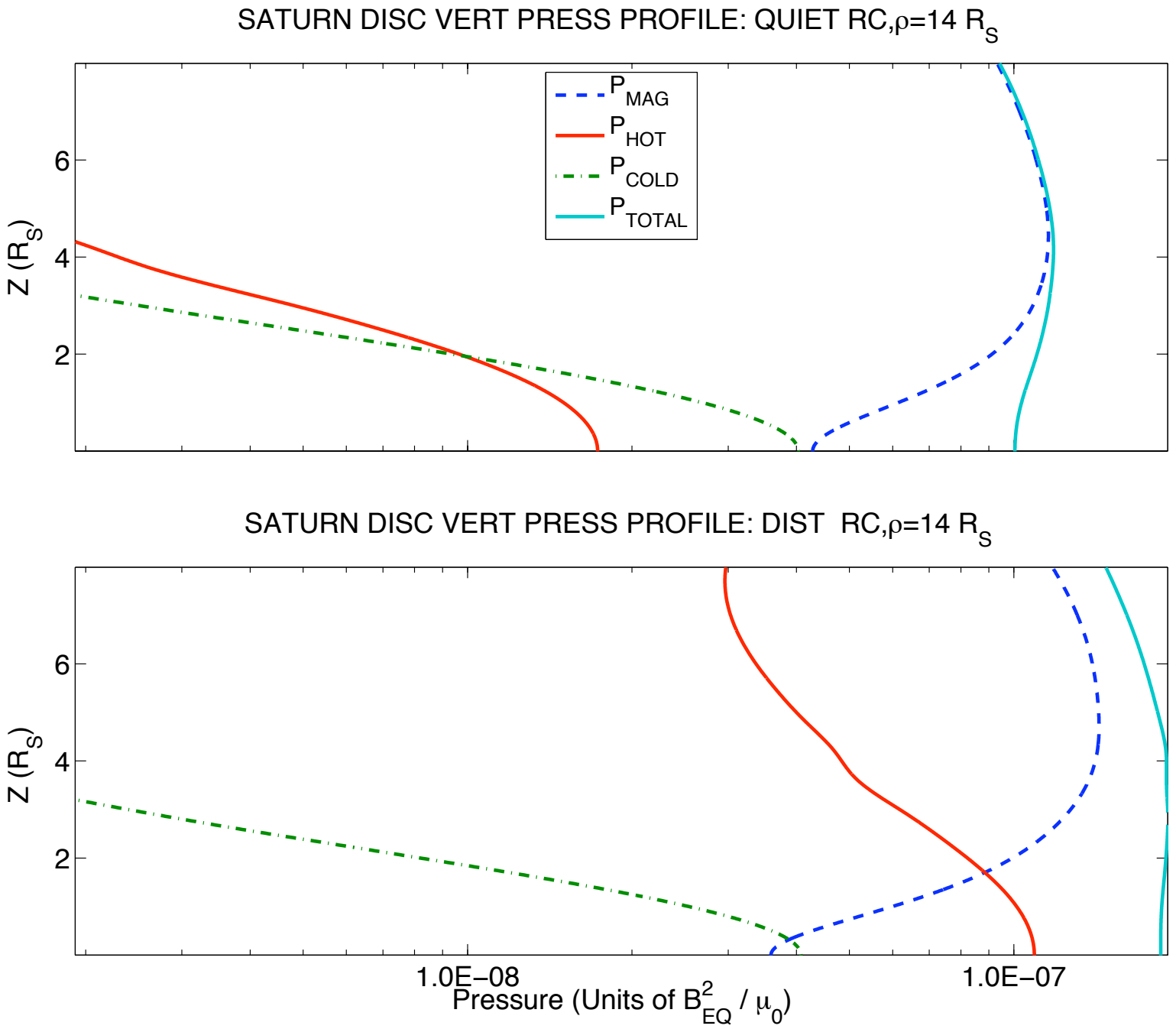

Figure 4, 'Vertical Pressure Profiles': We show relative pressures due to the equivalent magnetic force, hot plasma and cold plasma populations (for more details see Achilleos et al. (2010)). Pressure is shown as a function of vertical coordinate Z above the equatorial plane, at a constant cylindrical radial distance $\rho = 14R_S$. The 'disturbed' model shows the effect of increasing the hot plasma content as indicated by the red curves. The field develops into a more 'disc-like' configuration (Figure 3) which acts to more strongly confine the cold plasma and produce a thinner current sheet. The 'disturbed' model also shows a greater change in magnetic pressure between the current sheet (equatorial plane) and lobes (outside cold disc), in order to balance the increased vertical plasma pressure gradient.

Figure 5: Equatorial Fields and Radial Force Balance

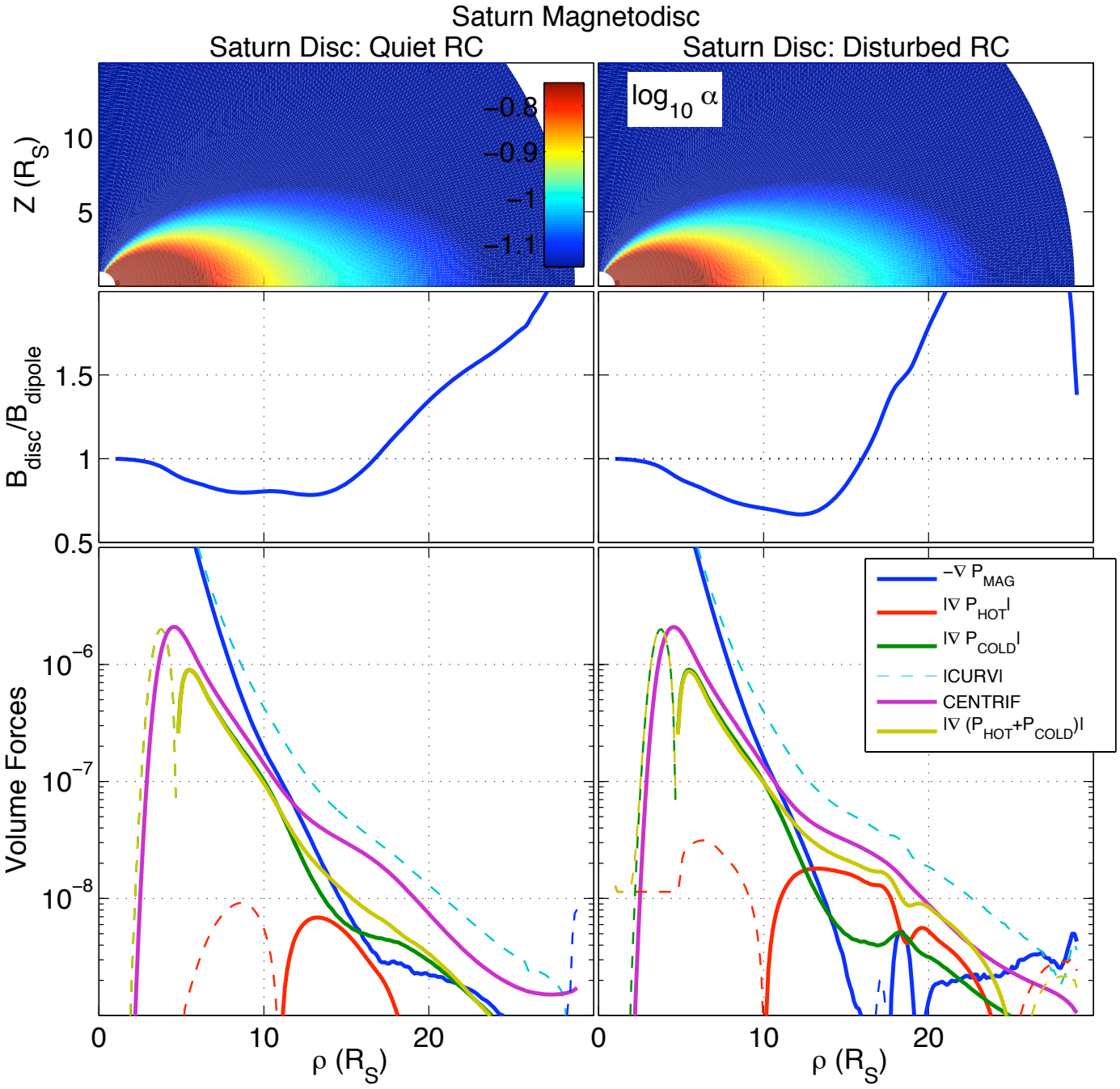

Figure 5, 'Equatorial Fields and Radial Force Balance': *Top Panels:* Contours (logarithmic) of constant magnetic potential α for the quiet and disturbed disc models. *Middle Panels:* Ratio of equatorial magnetic fields of the model (dipole plus disc) and planetary dipole (dipole alone). The hot disc contributes a stronger relative perturbation to the background dipole, especially in the region $> 18\ R_S$. *Bottom Panels:* Equatorial radial forces on a relative scale for both disc models, colour-coded according to physical origin. Solid lines show outward-directed force, while dashed lines denote forces which are inward-directed. We show magnetic curvature force, magnetic pressure gradient, plasma pressure gradients (hot and cold), and centrifugal force. Note that the outer magnetosphere ($>\sim 12\ R_S$) in the disturbed model is formed principally by a balance between magnetic curvature and a combination of centrifugal force and plasma pressure, while the plasma pressure gradients play a much less important role in the quiet disc model. The behaviour of the disturbed disc is more in agreement with the forces and currents derived from observations (e.g. Sergis et al. (2009), Kellett et al. (2009)).

Summary I

Magnetic Moments: The quiet and disturbed current disc models have respective magnetic moments of 0.58 μ_S and 0.52 μ_S, where μ_S is the planetary dipole moment, defined as:

$$\mu_S = 4\pi B_{EQ} R_S^3 / \mu_0, \tag{2}$$

where B_{EQ} denotes equatorial field strength at the planet surface. The fact that the planetary and disc moments are of similar order of magnitude indicates that the extension of the disc currents over a much larger spatial volume in a sense compensates for their weaker density relative to the internal planetary currents. We note that our theoretical values are also in good agreement with the results of Bunce et al. (2007), who determined ring current moments in the range 0.2–0.7μ_S through fitting Cassini magnetic data with a Connerney-type disc model. Additional calculations in progress reveal that we cannot obtain stable solutions for disc magnetic moments in excess of $\sim 1.5\ \mu_S$. We shall address the physical meaning of this result in a future study, but feel it is indicative of a 'stability limit' associated with the thermal energy content of a stable magnetosphere.

Summary II

General Properties:

- **A change in the internal magnetospheric plasma content is very likely to have an influence on field structure at Saturn.** A more 'disc-like' magnetic field configuration is required to maintain force balance with a system of higher hot plasma content. The external influence of solar wind pressure can also make Saturn's magnetospheric field change between 'dipole-like' and 'disc-like' states (e.g. Arridge et al. (2008), Bunce et al. (2007), Achilleos et al. (2010)).
- Increased hot plasma content leads to a stronger contrast between the magnetic field at the centre of the current sheet (equatorial plane in our model) and the 'lobe' regions outside the main current-carrying region.
- Depending on the global concentrations of hot plasma relative to the cold population, the force balance in Saturn's magnetosphere is principally determined by a balance between inward-directed magnetic curvature force and outward-directed centrifugal force and plasma pressure gradient, with the plasma pressure becoming less important for the 'quiescent' ring current state—a simplified representation of the hot plasma population we have used here, based on simple statistical characterisations along the lines of Sergis et al. (2007).

References

Achilleos N., Guio P., Arridge C. S., 2010, Mon. Not. Royal Ast. Soc., 401, 2349

Arridge C. S., Russell C. T., Khurana K. K., Achilleos N., Cowley S. W. H., Dougherty M. K., Southwood D. J., Bunce E. J., 2008, J. Geophys. Res., 113, 4214

Bunce E. J., Cowley S. W. H., Alexeev I. I., Arridge C. S., Dougherty M. K., Nichols J. D., Russell C. T., 2007, J. Geophys. Res., 112, 10202

Caudal G., 1986, J. Geophys Res., 91, 4201

Connerney J. E. P., Acuna M. H., Ness N. F., 1981, Nature, 292, 724

Kellett S., Bunce E. J., Coates A. J., Cowley S. W. H., 2009, J. Geophys. Res., 114, A04209

Krimigis S. M., Mitchell D. G., Hamilton D. C., Livi S., Dandouras J., Jaskulek S., Armstrong T. P., Boldt J. D., Cheng A. F., Gloeckler G., Hayes J. R., Hsieh K. C., Ip W.-H., Keath E. P., Kirsch E., Krupp N., Lanzerotti L. J., Lundgren R., Mauk B. H., McEntire R. W., Roelof E. C., Schlemm C. E., Tossman B. E., Wilken B., Williams D. J., 2004, Space Sci. Rev., 114, 233

Sergis N., Krimigis S. M., Mitchell D. G., Hamilton D. C., Krupp N., Mauk B. H., Roelof E. C., Dougherty M. K., 2009, J. Geophys. Res., 114, A02214

Sergis N., Krimigis S. M., Mitchell D. G., Hamilton D. C., Krupp N., Mauk B. M., Roelof E. C., Dougherty M., 2007, Geophys. Res. Lett., 34, L09102